Molecular Dynamics Simulation
of Argon
for AP3081 D

Bas Nijholt

March 3, 2014

Date started:	February 3, 2014
Instructor:	Dr. J.M. Thijssen

Abstract

Molecular Dynamics simulation is a technique for computing equilibrium and dynamic properties of a classical many-body system. Newtons equations of motion are solved numerically, and macroscopic properties of the system are measured by applying statistical mechanics principles. In this report, we will discuss the key ingredients in carrying out a molecular dynamics simulation. This includes the potentials used to model intermolecular interactions, the integration algorithms and the boundary conditions that are implemented. We will present the results of simulations performed for a system of 864 particles interacting through a Lennard-Jones potential, and interpret the results for argon.

1 Introduction

With computer simulation we study macroscopic systems which can not be solved analytically. This is done by implementing microscopic models which specify intermolecular interactions and molecular structure. The result from computer simulations can be compared with analytical predictions and experimental data to test the accuracy of the model. Molecular dynamics uses computer simulation with statistical mechanics to compute static and dynamic properties of a classical many-body system. Static properties include the energy, temperature and pressure of a system while dynamic properties include the diffusion coefficient and time correlation functions of a system. In our molecular dynamics simulations we first specify the initial positions and momenta of the particles. Then we evolve the system according to Newtons second law: $F_i = m_i \cdot a_i$ in which we let the particles interact through a Lennard-Jones potential. Finally we measure physical quantities as functions of particle positions and momenta. Statistical mechanics is used to interpret the static properties

such as temperature and pressure. The results obtained from the simulations are interpreted for argon for which the Lennard-Jones description has been very successful [6]. With our assay we aim to study macroscopic systems, but only a "small" finite number of particles can be simulated on a computer. Real systems contain $\mathcal{O}(10^{23})$ particles [1]. To mimic the bulk surrounding the sample, periodic boundary conditions are implemented. This and other considerations in setting up a molecular dynamics simulation, such as the integration algorithms are discussed in Chapter 2. In Chapter 3, results of computer simulations are presented. We will compare these results to the simulations done by Verlet in 1967 [9]. His data corresponds very well to experimental data [2, 4, 5].

1.1   Intermolecular Interactions

The intermolecular interactions are modeled by the 12-6 Lennard-Jones potential as in figure 1, which is typically used to model interactions between non-polar molecules. This potential is a function of the positions of the nuclei and depends only on the magnitude of the pair separation $r_{ij} = |\mathbf{r}_i - \mathbf{r}_j|$. We will only consider these pairwise interactions, since their contribution is most significant. The potential energy of the whole system is written as

$$U\left(\mathbf{r}^N\right) = \sum_i \sum_{i<j} \phi_{LJ}(r) \tag{1}$$

in which the Lennard-Jones potential ϕ_{LJ} is

$$\phi_{LJ}(r) = 4\epsilon \left[\left(\frac{\sigma}{r}\right)^{12} - \left(\frac{\sigma}{r}\right)^6 \right] \tag{2}$$

Here σ represents the effective diameter of the spherical particles and ϵ measures the attractive interaction as is indicated in figure 1. The potential consists of a short-range repulsive force $(1/r^{12})$ arising from screening effects and from Pauli's exclusion principle, and a long-range attractive force $(1/r^6)$ arising from van der Waals dispersion forces. In this report we choose $\sigma = \epsilon = 1$. The total intermolecular force is the gradient of the potential with respect to particle displacements.

$$\mathbf{F}_i = -\sum_{i\neq j} \frac{\partial \phi_{LJ}(r_{ij})}{\partial r_{ij}} = -24 \sum_{i\neq j} \left[2\left(\frac{1}{r_{ij}}\right)^{13} - \left(\frac{1}{r_{ij}}\right)^7 \right] \tag{3}$$

1.2   Boundary Conditions

Though we try to find information about a physical system, only a small number of particles is considered, while a real physical system contains many moles of particles $\mathcal{O}(10^{23})$ which is impossible to simulate exactly. Because we choose a system of 'only' 864 particles, the ratio of surface molecules to the molecules

---

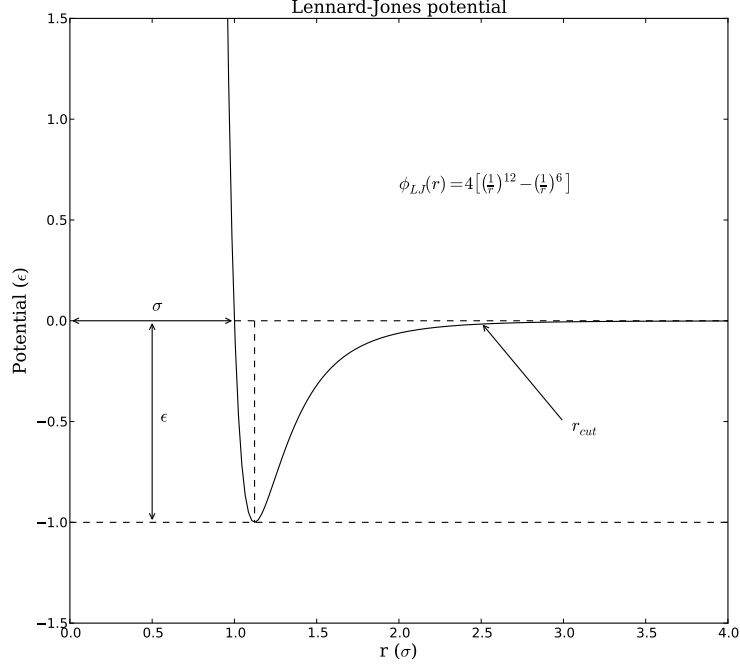[1]Avogadro's constant is $6.022 \cdot 10^{23}$ mol^{-1}

Figure 1: A graph of strength versus distance for the 12-6 Lennard-Jones potential with $\sigma = \epsilon = 1$ in which the significant parameters are depicted. The potential in cut at $r_{cut} = 2.5\sigma$ which is explained in the computation part of the report.

in bulk is higher than in reality. Therefore periodic boundary conditions are implemented, which mimics the behavior of the infinite bulk surrounding the sample. In this way surface effects are removed. In figure 2 one can see the difference in using a periodic or a hard wall boundary condition. It should also be noted that if the particles go through the wall, they will appear at the other side of the box.

1.3   Nearest-Neighbor Interaction

Using periodic boundary conditions solves the problem of surface effects, but gives rise to a new difficulty. Namely, we have $N = 864$ particles in a box, those particles do not only interact with each other, but also interact with particles in the periodic (mirrored) images. The short-range interactions of the Lennard-Jones potential are dominated by the interactions of the particles closer than a cut-off distance r_{cut}, as is indicated in figure 1. We choose a cut-off radius
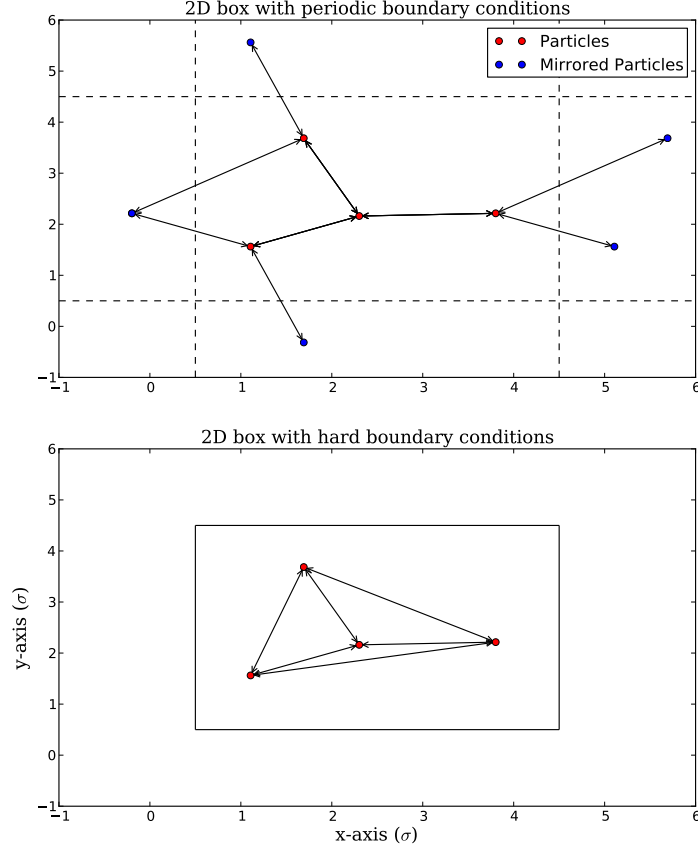
Figure 2: The choice of the type of boundary conditions (BCs) affects the properties of the system that is considered. In the figure hard walls and periodic BCs are compared. The top graph represents a two-dimensional system with periodic BCs and the graph at the bottom has hard walls as BCs. The arrows represent the pairwise interaction between two atoms. In the case of the periodic BCs, the nearest atom might not lie in the box itself, but an atom in a adjacent box (its mirror image) could be closer .

such that $r_{cut} \leq \frac{1}{2} L_{box}$. So the truncated potential becomes:

$$U(r) = \begin{cases} \phi_{LJ}(r), & r \leq r_{cut} \\ 0 & r > r_{cut} \end{cases} \qquad (4)$$

4

1.4 Equations of Motion

The classical equations of motion for the ith particle can be written as

$$m_i \ddot{\vec{x}}_i(t) = F_i(\vec{x}(t)) = -\nabla_{\vec{x}_i} \phi(\vec{x}(t)) \tag{5}$$

in which t is the time, $\vec{x}(t) = (\vec{x}_1(t), \ldots, \vec{x}_N(t))$ is the ensemble of the position vector of N particles, F is the force and ϕ is the scalar potential function, which is the Lennard-Jones potential in our case.

We can use finite difference methods to solve these differential equations approximately. In this report Verlet's velocity scheme is used, where positions, velocities and acceleration at time $t + \Delta t$ are obtained from the same quantities at time t in the following way:

$$\vec{x}(t + \Delta t) = \vec{x}(t) + \vec{v}(t)\,\Delta t + \frac{1}{2}\,\vec{a}(t)\Delta t^2 \tag{6}$$

$$\vec{v}(t + \Delta t) = \vec{v}(t) + \frac{\vec{a}(t) + \vec{a}(t + \Delta t)}{2}\Delta t \tag{7}$$

1.5 Reduced Units

In this report physical quantities are expressed as dimensionless or natural (reduced) units. This means that all quantities of interest are put to unity, so we do not work with very large or very small numbers. An advantage is that the equations of motion become simplified.

The following basic units are put to unity:

- length: $\sigma = 3.405\,\text{Å}$ for argon

- energy: $\epsilon = 119.8\,^\circ\text{K}$ for argon

- mass: $m = 39.9$ amu for argon[2]

- Boltzman's constant: $k_B = 1.381 \times 10^{-23}\,\text{J K}^{-1}$

Other derived reduced quantities are time $t^* = t\sqrt{\epsilon/m\sigma^2}$, pressure $P^* = P\sigma^3/\epsilon$, temperature $T^* = k_b T/\epsilon$, and density $\rho^* = \rho^3$.

For simplicity we will indicate the unit of time as Δt.

2 Computer Simulation

The simulations were constructed as follows:

1. Initialize particle positions and momenta.

---

[2] one amu is $1.660\,538\,92 \times 10^{-27}\,\text{kg}$

2. Compute forces on particles.

3. Integrate equation of motion.

4. Measure relevant quantities.

5. Repeat (2)-(4) for the designated period of time.

6. Compute averages.

2.1 Initialization

The particles are initiated at positions such that there is no overlap of the atomic cores. An easy way of doing this is placing the atoms on a lattice. For the simulations done in this report, we chose to place them on a face-centered cubic lattice for close packing as in figure 3. The lattice spacing was chosen to obtain the desired particle density.
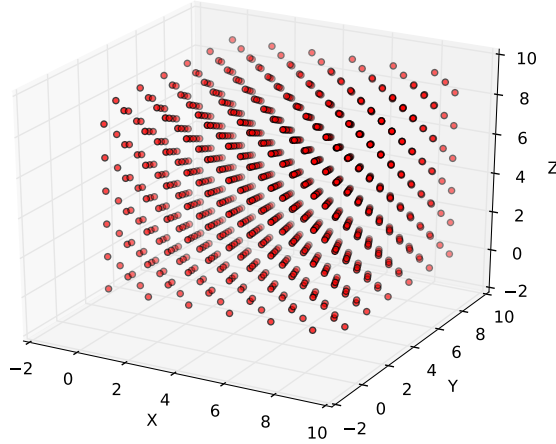

Figure 3: The atoms are initialy placed on a face-centered cubic lattice (FFC). The atom positions in the figure are depicted by the red points.

The initial velocities must satisfy the desired initial temperature[3]. They can be arbitrarily selected from the Maxwell-Boltzmann distribution

$$f(v) = \sqrt{\left(\frac{m}{2\pi kT}\right)^3} 4\pi v^2 \exp\left(-\frac{mv^2}{2kT}\right), \tag{8}$$

---

[3]Temperature and velocity are related as $\frac{1}{2}mv^2 = \frac{3}{2}k_B T$

In order to generate normally distributed numbers from uniformly distributed random numbers the Box-Muller transform is used

$$Z_0 = R\cos(\Theta) = \sqrt{-2\ln U_1}\cos(2\pi U_2) \tag{9}$$

in which U_1 and U_2 are uniformly distributed random numbers. The initial velocities that are generated have a very similar distribution as in the end of the simulation. This can be seen in figure 4, which also justifies the use of the Maxwell-Boltzmann distribution.
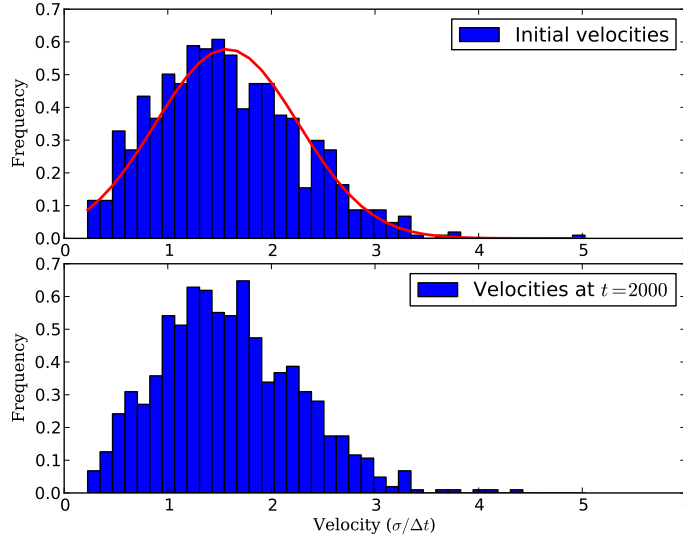

Figure 4: The initial velocities of the atoms are normally distributed (top histogram). The red curve is a Gaussian fit. After the simulation is done the distribution is still normally distributed (lower histogram).

2.2   Computing Forces

The force is the gradient of the Lennard-Jones potential (equation 3). So the force of the x-component on the ith particle is given by

$$f_{x_i}(r) = -\frac{\partial \phi_{LJ}(r)}{\partial x_i} = -\left(\frac{x_i}{r}\right)\left(\frac{\partial \phi_{LJ}(r)}{\partial r}\right) = \frac{48x_i}{r^2}\left[\frac{1}{r^{12}} - 0.5\frac{1}{r^6}\right] \tag{10}$$

2.3   Integration

We implemented Verlet's velocity scheme (equations 6 and 7) as follows:

1. calculate $\vec{v}(t + \Delta t) = \vec{v}(t) + \frac{1}{2}\vec{a}(t)\Delta t$

7

2. calculate $x + \vec{\Delta t}(t) = \vec{x}(t) + \vec{v}(t + \Delta t)\Delta t \pmod{L_{box}}$

3. derive $\vec{a}(t + \Delta t)$ from the interaction potential using $\vec{x}(t + \Delta t)$

4. calculate $\vec{v}(t + \Delta t) = \vec{v}(t + \Delta t) + \frac{1}{2}\vec{a}(t + \Delta t)\Delta t$

A time-step of $\Delta t = 0.004$ is used, unless indicated differently.

2.4 Measurements

The system must establish equilibrium before measurements can be made. The temperature is rescaled with a factor $\sqrt{T/T_0}$ for a certain time until the desired temperature (T_0) is reached as is shown in figure 5. After equilibrium is reached, the total energy is constant as can be seen in figure 6.
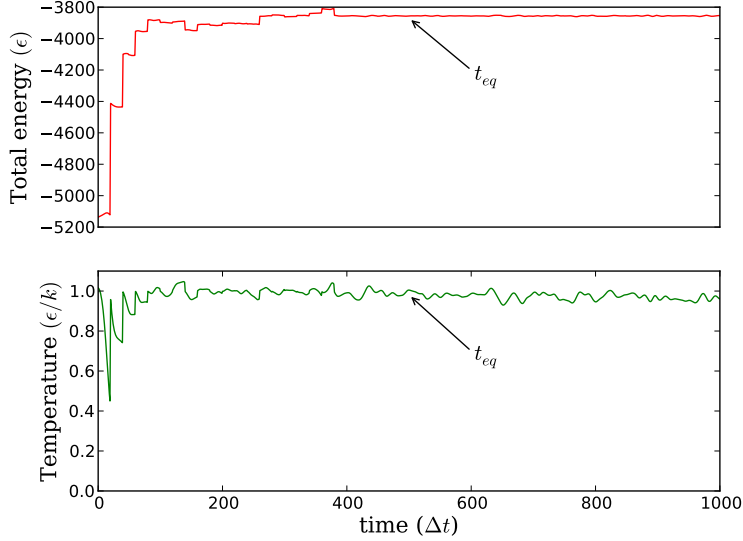
Figure 5: The temperature is rescaled every 20 time-steps until t_{eq}, which in this case $t_{eq} = 500$. We then assume the total energy constant. This system has a density $\rho = 0.85$.

The measurements involve time averages of a physical quantity A over the system trajectory

$$\langle A \rangle = \frac{1}{N} \sum_{i=1}^{N} A_i(t) \tag{11}$$

for N time-steps. The values $A_i(t)$ are considered as independent if one correlation time τ has past. The correlation time τ is found by calculating the

8

Figure 6: Equilibration phase for a system at $T = 1$ and $\rho = 0.85$. The potential and kinetic energy fluctuate about equilibrium values while the total energy is practically constant.

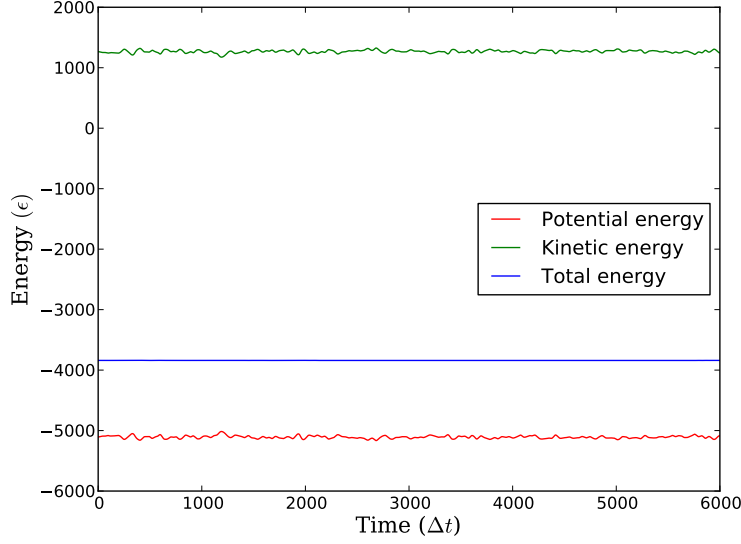auto-correlation function as in figure 7. The correlation time is defined as the time it takes for the autocorrelation function to have a factor of $1/e$ of its original value. The correlation time is $5 < \tau < 25$ depending on the system, so for safety $\tau = 50$ is used.

The averages are subject to systematic and statistical errors. Systematic errors are associated with numerical integration, finite size effects and the interaction cut-off. Statistical errors are due to random fluctuations in measurements. To make the values A_i values independent, block averaging [7] is used. Which means that the average over blocks of 50 successive values is taken and used to calculate the variance, so the variance of the averages gives a measure of the error.

The following physical properties were measured:

• **Energy:** The total energy in each time-step is measured. The total energy $E = K(t) + U(t)$ is conserved by classical Newtonian dynamics (figure 6). The potential energy $U(t)$ is given by equation 1 and the kinetic energy is

9

$$\hat{R}(k) = \frac{1}{(n-k)\sigma^2} \sum_{t=1}^{n-k}(X_t - \mu)(X_{t+k} - \mu)$$
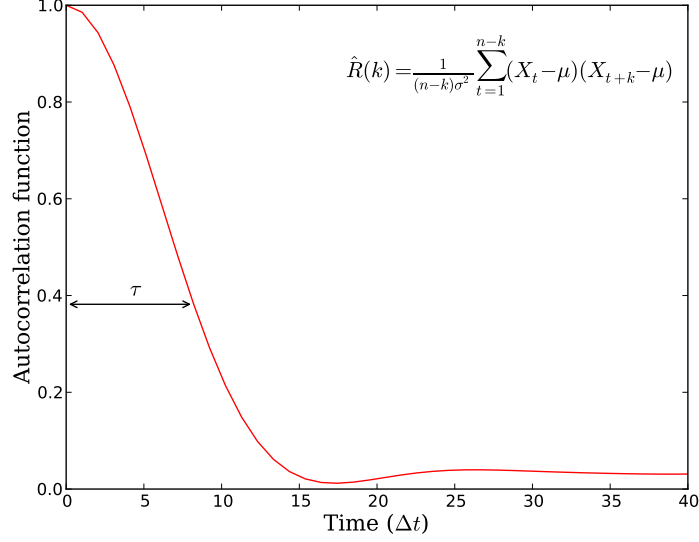
Figure 7: Time dependence of the estimated autocorrelation function. The correlation time τ is indicated, which is about 8 in this case.

$$K(t) = \frac{1}{2}\sum_{i=1}^{N}|v_i(t)|^2 \tag{12}$$

• **Temperature:** The instantaneous temperature is computed from the equipartition theorem which states that the kinetic energy equals $\frac{1}{2}Nk_BT$ per degree of freedom. In the case of argon

$$K = \frac{3}{2}Nk_BT \tag{13}$$

• **Pressure:** The pressure can be found in a simulation using the virial theorem [1, 8, 9]:

$$\frac{\beta P}{\rho} = 1 - \frac{\beta}{3N}\left\langle \sum_{i=1}^{N}\vec{r}_i\nabla_i\phi_{LJ}(r)\right\rangle \tag{14}$$

where $\langle\cdots\rangle$ denotes the time average and $\beta = 1/k_BT$. As the potential is truncated at $r_c = 2.5$, a correction term is needed. The correction term is

proportional to

$$-\frac{2\pi N\rho}{3k_BT}\int_{r_c}^{\infty}\frac{\partial\phi_{LJ}(r)}{\partial r}g(r)r^3dr = -\frac{16\pi\rho}{k_BT}\left(\frac{2}{9r_c^9}-\frac{1}{3r_c^9}\right)g(r) \approx \frac{16\pi\rho}{3k_BT}\frac{1}{r_c^3} \quad (15)$$

The replacement of $g(r)$ by 1 in the correction term leads, for $r_c = 2.5$ to a maximum error of 0.05.

- **Specific heat:** The specific heat can be found from the fluctuation of the kinetic energy from a formula derived by Lebowitz [3, 8]:

$$\frac{\langle\delta K^2\rangle}{\langle K\rangle^2} = \frac{2}{3N}\left(1 - \frac{3N}{2C_V}\right) \quad (16)$$

$$C_V = \frac{1}{\frac{2}{3N} - \frac{\langle\delta K^2\rangle}{\langle K\rangle^2}} \quad (17)$$

- **Chemical potential:** The chemical potential is calculted using the Widom insertion method [10] in which periodically a 'ghost' particle at a random position is inserted and subsequently the change in energy ΔU is measured that would result if the particle is actually placed. In our simulation we do such a trial each 50 time-steps, 10000 times. The chemical potential is related to the change in potential energy as

$$\mu = -k_BT\left\langle e^{\Delta U/k_BT}\right\rangle \quad (18)$$

where $\langle\cdots\rangle$ denotes the average over many random additions of the ghost particle.

- **Pair correlation function $g(r)$:** The static pair correlation function $g(r,r')$ is proportional to the probability of finding a particle at r from any other particle r', so it describes how density varies as a function of distance from a reference particle. In the canonical ensemble it is given by

$$g(r) = \frac{1}{4\pi N\rho r^2}\left\langle\sum_{i\neq j}\delta(r - r_{ij})\right\rangle \quad (19)$$

- **Diffusion coefficient:** The diffusion coefficient is related to the variance of the square of the displacement $\langle r^2\rangle$ as

$$\langle r^2\rangle = 6Dt \quad (20)$$

The total displacement is recorded during a simulation after equilibrium has been reached. Since the dependence of D on t is linear, we have used the method of least squares the estimate the diffusion coefficient.

3 Results

The over-all agreement between our simulation and experimental data is very good. In figure 8 the compressibility factor $\beta P/\rho$ is plotted and compared with the data computed by Verlet [9]. The errors are in the order of 0.05.
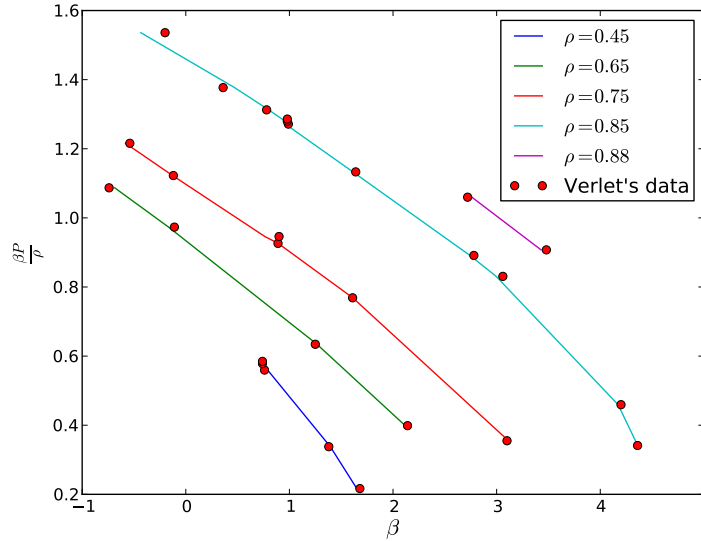
Figure 8: The compressibility factor $\beta P/\rho$ as a function of β for isochores $\rho = 0.88$, 0.85, 0.75, 0.65 and 0.45 (solid colored lines), and compared with the data computed by Verlet [9]. The red dots that overlap with the lines correspond to measurements of the same density.

In figure 9 the results of the measurements of the specific heat are plotted as a function of temperature. The data corresponds to what we would expect in high density, low temperature and low density, high temperature situations, respectively the Dulong-Petit law and the specific heat for a ideal gas at high temperature. The errors are in the order of 50 to 100.

With the method of least squares we calculated the diffusion coefficient D and found a corresponding error of 0.1%. For $\rho = 0.85$ the diffusion coefficient is plotted as a function of temperature and pressure in figure 10. The diffusion coefficients we measured for other densities can be found in table 1.

The chemical potential we measured can be found in table 1. The chemical potential goes down very rapid on increasing temperature and consequently pressure. This is what was expected, as it is 'costs' more energy to add a par-
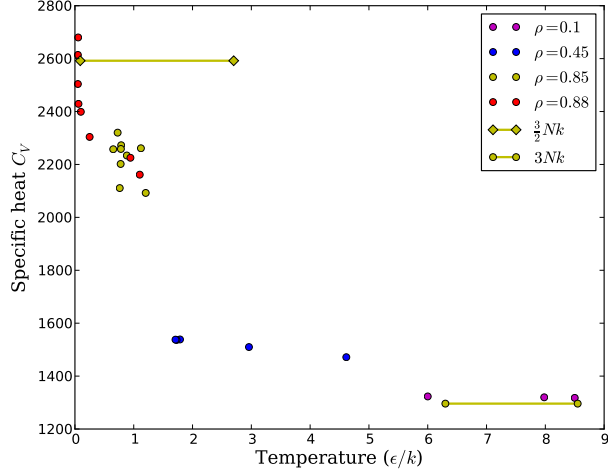
Figure 9: The specif heat as a function of temperature. The specific heat that we expect at high density, low temperature and low density, high temperature systems, respectively the Dulong-Petit law and the specific heat for a ideal gas at high temperature are similar to what is measured.
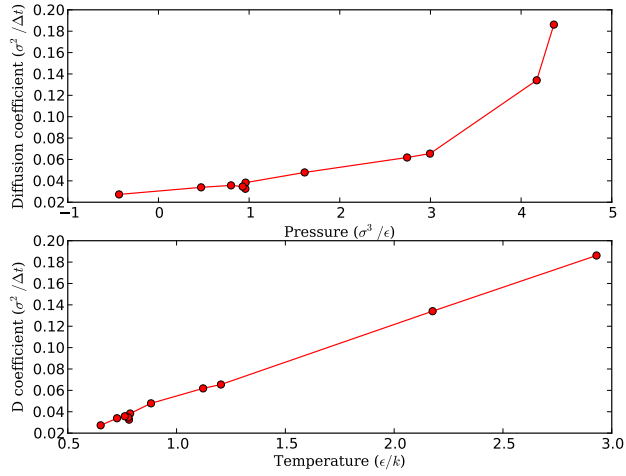
Figure 10: Diffusion coefficient as a function of pressure (top) and temperature (bottom) for $\rho = 0.85$.

ticle to the system. The error in these measurements varies from 3 to 25 %.

13

Table 1: List of thermodynamical results: ρ is the particle density, T_0 is the preset temperature, and T is the average temperature of the system, $\beta P/\rho$ is the compressibility factor, μ is the chemical potential, C_V is the specific heat and D is the diffusion coefficient. The units can easily be derived from the reduced units given in section 1.5.

| ρ	T_0	T	U	$\beta P/\rho$	μ	C_V	D
0.45	4.63	4.62	4079	1.65	-1.5584650	1471	0.844
0.45	2.94	2.96	1629	1.39	-0.5454923	1510	0.673
0.45	1.76	1.79	-156	0.79	-0.1087776	1539	0.436
0.45	1.74	1.73	-245	0.75	-0.0953481	1537	0.446
0.45	1.71	1.71	-281	0.71	-0.0918470	1538	0.413
0.65	2.56	2.51	20	2.12	-0.1401748	1644	0.297
0.65	1.59	1.58	-1560	1.27	-0.0162097	1789	0.203
0.65	1.04	1.03	-2531	-0.17	-0.0009151	1825	0.136
0.65	0.90	0.92	-2731	-0.69	-0.0003651	1809	0.128
0.75	2.85	2.82	209	3.11	-0.1468995	1740	0.237
0.75	1.30	1.30	-2570	1.61	-0.0022013	2050	0.115
0.75	1.07	1.08	-2997	0.89	-0.0004953	1856	0.099
0.75	1.07	1.06	-3046	0.76	-0.0004050	1927	0.097
0.75	0.88	0.89	-3375	-0.13	-0.0000787	2034	0.079
0.75	0.83	0.82	-3509	-0.58	-0.0000331	2005	0.068
0.85	2.89	2.93	225	4.36	-0.1187017	1916	0.186
0.85	2.20	2.18	-1238	4.17	-0.0289495	1982	0.134
0.85	1.21	1.20	-3223	3.00	-0.0004889	2092	0.065
0.85	1.13	1.12	-3398	2.74	-0.0002528	2261	0.062
0.85	0.88	0.88	-3927	1.61	-0.0000201	2234	0.048
0.85	0.79	0.79	-4138	0.96	-0.0000050	2273	0.038
0.85	0.78	0.78	-4143	0.96	-0.0000045	2259	0.033
0.85	0.78	0.78	-4154	0.93	-0.0000043	2202	0.035
0.85	0.76	0.76	-4188	0.80	-0.0000033	2111	0.036
0.85	0.72	0.73	-4270	0.47	-0.0000017	2320	0.034
0.85	0.66	0.65	-4448	-0.43	-0.0000003	2257	0.027
0.88	1.10	1.10	-3558	3.43	-0.0001595	2161	0.050
0.88	0.94	0.94	-3921	2.76	-0.0000317	2225	0.039

We can say something about the state of the system by measuring the static pair correlation function (PCF). In figure 11 the PCF is plotted as a function of distance to a reference particle for different temperatures.
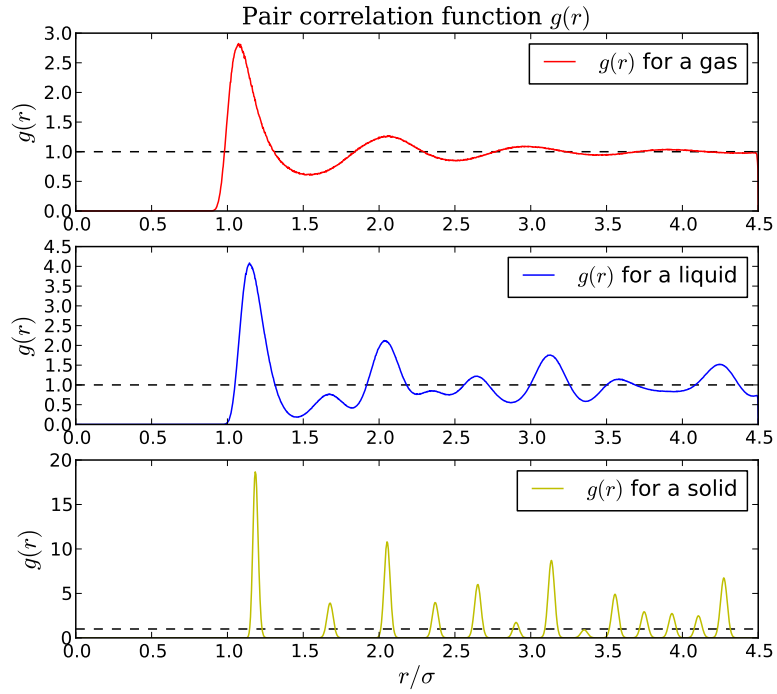
Figure 11: The static pair correlation (PCF) function as a function of distance to a reference particle. In the PCF one can see how many neighbors an particle has, and thus the density around a particle. At the top is a PCF for a gas ($T = 1$ and $\rho = 0.85$), which has a uniform density after a certain distance. In the middle a PCF for a liquid ($T = 0.3$ and $\rho = 0.85$) and at the bottom for a solid ($T = 0.01$ and $\rho = 0.85$). The first peak indicates its 12 nearest neighbors in the fcc and the second peak its 6 next nearest neighbors.

4 Conclusions

It can be concluded that the Lennard-Jones potential represents the behavior of argon and with it one can predict the equilibrium properties of argon by integrating relatively easy equations. The striking result [4] is the over-all agreement with experimental data of real argon.

References

[1] Jean-Pierre Hansen and I. R. McDonald. *Theory of Simple Liquids, Third Edition*. Academic Press, 3 edition, April 2006.

[2] A. Van Itterbeek, O. Verbeke, and K. Staes. Measurements on the equation of state of liquid argon and methane up to 300 kg cm2 at low temperatures. *Physica*, 29(6):742 – 754, 1963.

[3] J.L. Lebowitz, J.K. Percus, and L. Verlet. Ensemble dependence of fluctuations with application to machine computations. *Physical Review*, 153(1):250–254, 1967. cited By (since 1996)144.

[4] J.M.H. Levelt. The reduced equation of state, internal energy and entropy of argon and xenon. *Physica*, 26(6):361 – 377, 1960.

[5] A. Michels, Hub Wijker, and Hk Wijker. Isotherms of argon between 0c and 150c and pressures up to 2900 atmospheres. *Physica*, 15(7):627 – 633, 1949.

[6] A. Rahman. Correlations in the motion of atoms in liquid argon. *Phys. Rev.*, 136:A405–A411, Oct 1964.

[7] D. C. Rapaport. *The Art of Molecular Dynamics Simulation*. Cambridge University Press., 2004.

[8] J.M. Thijssen. *Computational Physics*. Cambridge University Press, 2007.

[9] Loup Verlet. Computer "experiments" on classical fluids. i. thermodynamical properties of lennard-jones molecules. *Phys. Rev.*, 159:98–103, Jul 1967.

[10] B. Widom. Some topics in the theory of fluids. *Journal of Chemical Physics*, 39:2808–2812, December 1963.

---

[4]actually not really surprising, as many others before me did the same thing, but nonetheless...

5 Appendix

5.1 Remarks

It should be noted that I made all the plots in this report myself, and most of them are very dynamic. For example, the boundary condition plot (Fig. 2) has as input 'number of particles' and then randomly places the particles and draws the lines. The plot of the autocorrelation function automatically finds the closest value to $1/e$ in the array of the autocorrelation function, and draws the corresponding line. All plots are in vector form and made with the matplotlib library for Python. All of the 'hardcore' calculations are done in Fortran which writes the results to some files. These files are read with a Python program in which all the data analysis is done. I'm sorry for exceeding the four page limit you requested, I got a bit excited...

5.2 The use of my program

Attached to this report is a .zip-file that contains my program. The Fortan part is called *md.f90* in which you can edit the input parameters in the first lines. After compiling and running the program with the command: *make; ./md*, four files are created,*data.dat, histogram.dat, mu.dat* and *array.dat*.

Open your favorite command shell to run the Python program *an.py* which prints some results. You can then enter the commands:
plot_pressure(), plot_pcf(), plot_energy(), plot_temperature() or *plot_autocorrelation()*.

In the folder *plots* you can find all the scripts to generate the other plots in this report.

5.3 Data

Tables with all the measurements used in the report[5].

---

[5]can also be found in *data/data.ods*

Ref. #	Time steps	ρ	T_0	T	T error	U	U error
1	10000	0.45	4.63	4.6152	0.000693	4079.5	0.1295
2	10000	0.45	2.94	2.9597	0.000519	1628.5	0.0738
3	10000	0.45	1.76	1.7870	0.000294	-156.0	0.0266
4	10000	0.45	1.74	1.7288	0.000186	-244.6	0.0277
5	10000	0.45	1.71	1.7102	0.000214	-281.5	0.0337
6	6000	0.65	2.56	2.5081	0.000317	19.7	0.0799
7	6000	0.65	1.59	1.5766	0.000382	-1560.5	0.0487
8	8000	0.65	1.04	1.0275	0.000203	-2530.7	0.0367
9	6000	0.65	0.90	0.9200	0.000208	-2730.8	0.0234
10	8000	0.75	2.85	2.8167	0.000422	208.9	0.0761
11	8000	0.75	1.30	1.3009	0.000465	-2569.9	0.0420
12	8000	0.75	1.07	1.0798	0.000249	-2996.8	0.0285
13	10000	0.75	1.07	1.0570	0.000314	-3046.2	0.0230
14	10000	0.75	0.88	0.8909	0.000237	-3375.2	0.0168
15	10000	0.75	0.83	0.8225	0.000136	-3509.0	0.0185
16	5000	0.85	2.89	2.9298	0.000765	225.5	0.1126
17	3000	0.85	2.20	2.1766	0.000650	-1237.8	0.1391
18	8000	0.85	1.21	1.2038	0.000265	-3223.1	0.0447
19	3000	0.85	1.13	1.1220	0.000241	-3398.5	0.0733
20	3000	0.85	0.88	0.8826	0.000230	-3926.7	0.0645
21	6000	0.85	0.79	0.7865	0.000127	-4137.6	0.0160
22	6000	0.85	0.78	0.7815	0.000264	-4143.4	0.0272
23	5000	0.85	0.78	0.7776	0.000171	-4154.1	0.0215
24	6000	0.85	0.76	0.7619	0.000147	-4187.6	0.0204
25	10000	0.85	0.72	0.7262	0.000176	-4269.8	0.0189
26	8000	0.85	0.66	0.6511	0.000168	-4447.5	0.0342
27	8000	0.88	1.10	1.1021	0.000271	-3557.8	0.0424
28	8000	0.88	0.94	0.9436	0.000295	-3921.1	0.0379

Ref. #	P	P error	K	K error	μ	μ error
1	1.65	0.000098	5981.25	0.90	-1.5584650	0.0320396
2	1.39	0.000069	3835.75	0.67	-0.5454923	0.0131166
3	0.79	0.000034	2315.93	0.38	-0.1087776	0.0045889
4	0.75	0.000027	2240.56	0.24	-0.0953481	0.0046138
5	0.71	0.000036	2216.39	0.28	-0.0918470	0.0037221
6	2.12	0.000141	3250.51	0.41	-0.1401748	0.0076038
7	1.27	0.000065	2043.34	0.50	-0.0162097	0.0012737
8	-0.17	0.000233	1331.66	0.26	-0.0009151	0.0001072
9	-0.69	0.000376	1192.29	0.27	-0.0003651	0.0000557
10	3.11	0.000318	3650.43	0.55	-0.1468995	0.0091052
11	1.61	0.000220	1686.01	0.60	-0.0022013	0.0002915
12	0.89	0.000025	1399.38	0.32	-0.0004953	0.0000713
13	0.76	0.000071	1369.90	0.41	-0.0004050	0.0000660
14	-0.13	0.000301	1154.58	0.31	-0.0000787	0.0000137
15	-0.58	0.000268	1065.95	0.18	-0.0000331	0.0000059
16	4.36	0.000884	3797.07	0.99	-0.1187017	0.0077077
17	4.17	0.000947	2820.82	0.84	-0.0289495	0.0026262
18	3.00	0.000434	1560.11	0.34	-0.0004889	0.0000745
19	2.74	0.000381	1454.13	0.31	-0.0002528	0.0000422
20	1.61	0.000156	1143.79	0.30	-0.0000201	0.0000034
21	0.96	0.000006	1019.37	0.16	-0.0000050	0.0000012
22	0.96	0.000014	1012.79	0.34	-0.0000045	0.0000011
23	0.93	0.000016	1007.82	0.22	-0.0000043	0.0000009
24	0.80	0.000038	987.39	0.19	-0.0000033	0.0000008
25	0.47	0.000128	941.19	0.23	-0.0000017	0.0000005
26	-0.43	0.000374	843.80	0.22	-0.0000003	0.0000001
27	3.43	0.000604	1428.26	0.35	-0.0001595	0.0000255
28	2.76	0.000548	1222.85	0.38	-0.0000317	0.0000059

Ref. #	C_V	t_{eq}	P_{verlet}	Δt	D	D error
1	1471	6000	1.68	0.004	0.8440	0.0247
2	1510	6000	1.38	0.004	0.6730	0.0136
3	1539	6000	0.76	0.004	0.4362	0.0093
4	1537	6000	0.74	0.004	0.4460	0.0080
5	1538	6000	0.74	0.004	0.4133	0.0142
6	1644	3000	2.14	0.004	0.2969	88.0962
7	1789	3000	1.25	0.004	0.2028	53.4799
8	1825	6000	-0.11	0.004	0.1358	31.4946
9	1809	3000	-0.74	0.004	0.1278	20.0718
10	1740	5000	3.1	0.004	0.2367	0.0040
11	2050	5000	1.61	0.004	0.1147	0.0030
12	1856	5000	0.89	0.004	0.0993	0.0024
13	1927	5000	0.9	0.002	0.0974	0.0056
14	2034	5000	-0.12	0.002	0.0787	0.0016
15	2005	5000	-0.54	0.002	0.0683	0.0022
16	1916	500	4.36	0.004	0.1862	0.0134
17	1982	500	4.2	0.004	0.1341	0.0072
18	2092	3000	3.06	0.004	0.0655	0.0046
19	2261	500	2.78	0.004	0.0619	0.0031
20	2234	500	1.64	0.004	0.0479	0.0027
21	2273	1500	0.99	0.004	0.0383	0.0039
22	2259	1500	0.98	0.004	0.0326	0.0019
23	2202	1000	0.98	0.004	0.0346	0.0032
24	2111	2000	0.78	0.004	0.0358	0.0021
25	2320	6000	0.36	0.003	0.0339	0.0010
26	2257	3000	-0.2	0.004	0.0273	0.0033
27	2161	5000	3.48	0.004	0.0505	0.0015
28	2225	5000	2.72	0.004	0.0385	0.0015